Chapter 3

Theoretical Description of Beta Decay Spectrum

To obtain a measure of the Fierz term, the beta decay spectrum must be precisely described. The description of the beta decay spectrum is written as a series of corrections on top of the main phase space factor. Through out this chapter, $\hbar = c = 1$.

The beta decay spectrum shape can be broken up in three different sections. The three terms are written out in equation 3.1

$$Q(E) = PS(E) * C(E) * (1 + b_{gt}\frac{m_e}{E}) \tag{3.1}$$

where $Q(E)$ is the total beta decay energy spectrum, $PS(E)$ is the phase space of the electron, $C(E)$ are all the hadronic and electromagnetic corrections multiplied together, and b_{gt} the Fierz term. This chapter will describe all that goes into the determining the beta decay spectrum.

3.1 Experimental Input to Describe Beta Decay

The corrections depend on several parameters of the decay. Some of them are just numbers, such as the atomic number of the daughter or mother nucleus or the mass number of the

system. However, there are two important parameters that are experimental measurements.

One is the q-value of the decay, which is defined in equation 3.2.

$$Q = m_{20_F} - (m_{20_{Ne}} + E_{level}) \tag{3.2}$$

where Q is the q-value, m_{20_F} is the nuclear mass of ^{20}F, $m_{20_{Ne}}$ is the nuclear mass of ^{20}Ne, and E_{level} is the energy of the 1.6 MeV nuclear state in ^{20}Ne. Since it is difficult to measure bear nuclei, the atomic masses are used. For ^{20}F, $m_{20Ne} = 19.9924401762(17)amu$, $m_{20F} = 19.999981252(31)amu$ [22] , and $E_{level} = 1.633674(15)MeV$ [20] . However, to get the total energy, m_e has to be added to the difference of atomic masses.

This mass difference is not quite the maximum electron energy. To get to the maximum electron energy, E_0, the energy of the recoiling nucleus has to be taken into account. The formula is shown in equation 3.3

$$E_0 = Q\frac{1 + \frac{m_e^2}{2MQ}}{1 + \frac{Q}{2M}} \tag{3.3}$$

with m_e is the electron mass and M is the average nuclear mass [12].

The other parameter is the charge radius of the daughter nucleus. There are several ways to calculate the charge radius. In this work, the charge radius was taken from the measured root mean square (RMS) charge radius and converted. It was assumed that the ^{20}Ne nucleus was a sphere. From this, the radius was calculated using equation 3.4

$$r = \sqrt{\frac{5}{3}} r_{rms} \tag{3.4}$$

where r_{rms} is the root mean square charge radius, and r the charge radius. For this

work, $r_{rms} = 3.0055(21)$ [3]

With the two parameters, the q-value and the phase space, the shape of all beta decay spectra can be described.

3.2 Phase Space Beta Decay

The main part of the beta decay spectrum is the phase space factor. It is shown in equation 3.5

$$\frac{dN}{dE} = C * p_e W (Q - W)^2 \tag{3.5}$$

were C is a constant which includes the matrix element squared, p_e is the electron momentum, W the total electron energy, and Q the q-value of the beta decay. This is derived from the density of states of the particle. The constant is where the Fierz term enters. This comes in from Fermi's Golden Rule, which is shown in equation 3.6.

$$\lambda = \frac{2\pi}{\hbar} \|M\|^2 \rho \tag{3.6}$$

where λ is the transition probability, M the matrix element, and ρ the density of the states. The main effect on the spectrum shape originates from the density of states. The number of states for both the electron and the neutrino is show in equation 3.7

$$N = \frac{1}{(2\pi\hbar)^6} \int dr_e^3 \int dp_e^3 \int dr_{\nu e}^3 \int dp_{\nu e}^3 \tag{3.7}$$

where r and p corresponds to the position and momentum of the electron (e) and the neutrino (ν_e). Doing the integral over both r's give two factors of the volume, which disappear

when the next factor is introduced. Since the neutrinos are unmeasured, the momentum of the neutrinos is integrated over. Assuming spherical symmetry, the new integral is shown in equation 3.8

$$dN = \frac{V^2}{4\pi^4\hbar^6} p_e^2 dp_e p_{\nu_e}^2 dp_{\nu_e} \tag{3.8}$$

This is simplified by approximating the neutrino as mass-less. The momentum of the neutrino is then equal to the energy of the neutrino. Then, the total energy E is written as a sum of the neutrino energy (or momentum) and the beta energy. Plugging that in gives equation 3.9 after integrating over the neutrino degrees of freedom.

$$dN = \frac{V^2}{4\pi^4\hbar^6} (E - E_e)^2 p_e^2 dp_e \tag{3.9}$$

Then, the only thing left to do to recover equation 3.5 is to rewrite dp in terms of dE. The energy E_e has been replaced with W, which is the energy of the electron divided by the mass an electron, and E has been replaced by the Q-value. Since the measurement is not an absolute one, but only concerned with the shape of the spectrum, the normalization factor is arbitrary.

This is the main factor in describing the beta decay energy spectrum.

3.3 Variables of Correction Formula

For the rest of the discussion on beta decay corrections, everything is given without units. These corrections are largely electromagnetic in origin. All of the energies are divided by the electron mass. For this work, $m_e = 0.510998928 MeV$ The other important variables are

shown in table 3.1

Table 3.1: Variables used in the theory corrections

Variable	Description	Equation or Value
A	Mass number	20
Z	Atomic number of daughter	10
α	Fine structure constant	1/137.0359
R	Root mean square charge radius of daughter	3.055 fm [3]
W	Total energy of beta electron	E/m_e
p	Electron momentum	$\sqrt{W^2-1}$
W_0	Maximum electron energy	$\frac{E_0}{m_e}$
M_{ave}	Average nuclear mass	$\frac{M_{20Ne}+M_{20F}-19m_e}{2m_e}$
γ	Special relativity γ factor	$\sqrt{1-(\alpha Z)^2}$

Before the theoretical corrections were fed into a Monte Carlo simulation, the uncertainties from the experimentally determined quantities was checked. Theoretical spectra were built with each value plus or minus it's uncertainty. Ratios between the spectra were taken and fit with a line. The results of those ratios are seen in figure 3.1.

Since the slopes of each line are much smaller than the shape factor values, the experimental uncertainties are negligible. The various theoretical corrections that are needed are now discussed below.

3.4 Electromagnetic Corrections and Hardonic Corrections

A graph of the various electromagnetic corrections are shown in figure 3.2, along with the hadronic shape factor.

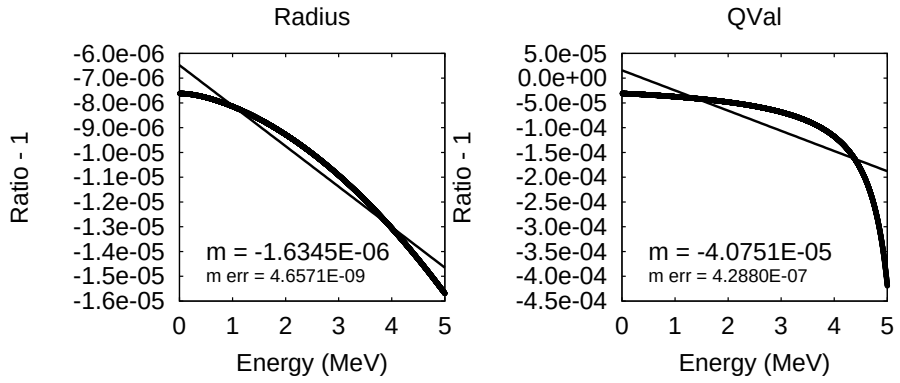

Figure 3.1: An estimate of the theory uncertainty due to the experimental parameter uncertainty. Shown are the slopes for each experimental parameter. They are orders of magnitude smaller than the 10^{-2}/MeV of the C_1.

3.4.1 Fermi Function

The largest correction by over all size is the Fermi function. This accounts for the interaction of the charge of the outgoing electron and the charge of the nucleus. It is calculated by taking the Dirac equation wave functions and assuming the nucleus is a point charge of Ze. The Dirac wave functions are taken down to a nuclear radius R. This is since the wave functions diverge [26].

The Fermi function is printed in equation 3.10

$$F(Z,W) = 2\frac{\gamma+1}{\Gamma(2\gamma+1)^2}(2pR)^{2(\gamma-1)}e^{\frac{\pi\alpha ZW}{p}}\|\Gamma(\gamma+i\frac{\alpha ZW}{p}\|^2 \tag{3.10}$$

While this is the largest correction, it is the most understood one. The change of shape

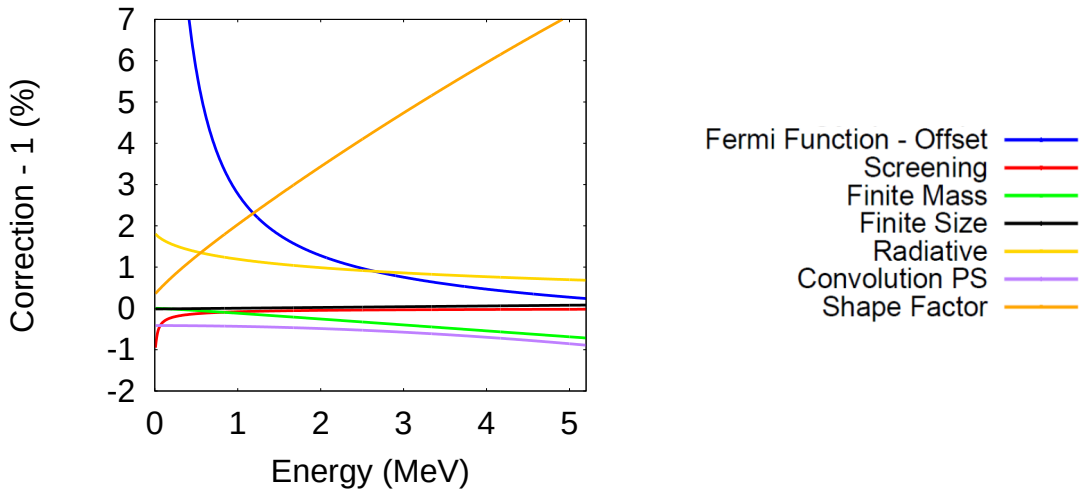

Figure 3.2: All the electromagnetic and hardonic corrections for ^{20}F plotted.

due the uncertainty in R is very small due to the functional form of the Fermi function.

3.4.2 Radiative Correction

The radiative correction was the next largest electromagnetic correction. For this measurement, the correction is only need to first order, which is on order α. The correction is a QED correction that stems from photons emitted from the beta particle. This photon can be absorbed by the nucleus of the daughter, which makes it a virtual photon. The photon can also be a real photon that propagates out off to infinity. The real photons are known as inner bremsstrahlung.

There are different descriptions of the radiative correction. The first is by Sirlin [19] and is shown in equation 3.11.

$$\begin{aligned} \mathrm{R(W,W_0)} = 1 + \frac{\alpha}{2\pi}[3ln(M) - \frac{3}{4} + 4(\frac{arctanh(\beta)}{\beta} - 1) * (\frac{W_0 - W}{3W} - \frac{3}{2} + ln(2(W_0 - W))) \\ + \frac{4}{\beta}L(\frac{2\beta}{1+\beta}) + \frac{arctanh(\beta)}{\beta} * (2 * (1 + \beta^2) + \frac{(W_0 - W)^2}{6W^2} - 4arctanh(\beta)] \end{aligned} \tag{3.11}$$

with $\beta = \frac{p}{W}$, M the proton mass, and $L(\frac{2\beta}{1+\beta})$ referening to the Spence function, as seen in equation 3.12 [28]

$$L(x) = \int_0^x \frac{ln(1-t)}{t} dt \tag{3.12}$$

The Sirlin formula assumes that the inner bremsstrahlung photons are not detected at all. This is mostly true if the source of the beta decay is centered outside of a detector. However, if the source is implanted inside of the detector, such as it is in this experiment, some of the inner bremsstrahlung is absorbed.

If all the inner bremsstrahlung is absorbed, a different form of the first order radiative correction is needed. There are many equivalent forms of this, but the one that was used for this experiment was by Fayans [7]. The form of this radiative correction is shown in equation 3.13

$$\begin{aligned} \mathrm{R(W,W_0)} = 1 + \frac{\alpha}{\pi}[(\frac{2}{\beta}ln(\frac{2\beta}{1+\beta}) + \frac{7}{8\beta} + \frac{3\beta}{8})ln(\frac{1+\beta}{1-\beta}) \\ - 2ln(\frac{4\beta^2}{1-\beta^2}) + \frac{4}{\beta}L(\frac{2\beta}{1+\beta}) + \frac{23}{8} + \frac{3}{2}ln(M)] \end{aligned} \tag{3.13}$$

With all the functions and variables meaning the same as in equation 3.11.

Unfortunately, the amount of inner bremssstrahlung absorbed depends on the geometry. A more careful treatment of the radiative correction is needed.

3.4.2.1 Inner Bremmsstrahlung

To first order, the energy spectrum of the inner bremsstrahlung photons is independent of Z. This is exactly like the two radiative corrections shown in equations 3.11 and 3.13. The spectrum is written out in equation3.14 [15]

$$\Phi(k, W_e) = \frac{\alpha p}{\pi p_e k}(\frac{W_e^2 + W^2}{W_e p} log(W + p) - 2) \tag{3.14}$$

where $\Phi(k, W_e)$ is the probability density of seeing a photon of energy k from an electron of initial energy W_e. This equation was derived one way using outgoing waves from the Dirac equation in polar coordinates. This was calculated with the first order Born approximation. This means that at low energies, equation 3.14 is inaccurate. That can be seen, as the equation diverges as k goes to zero. If more orders of the approximation are added, this divergence can be controlled. These higher orders would correspond to emitting multiple photons. Each of these orders would have a probability reduced by a factor of α compared to equation 3.14. The higher orders would be less significant, expect for at low energies. Since the probability density diverges, the higher orders could contribute. This would make the probability of emitting no photons finite.

However, another possibility is to add a cutoff. As long as the cutoff is high enough to be in the region where the first order Born approximation is valid, but low enough not to cut out gamma rays that are not full absorbed, equation 3.14 is usable. The cutoff used was 50 keV. This cutoff was checked using Monte Carlo, and is within the region where the detector

and the source geometry absorbs all gamma rays.

To quantify the exact effect of the inner bremsstrahlung, a GEANT4 simulation was used. Electrons were generated using the phase space and the radiative correction in equation 3.13. Then, for each electron, equation 3.14 was sampled and a photon generated. No other physics process was looked at in this simulation. The ratio consisting of the energy absorbed over the initial energy was the output of the simulation. That ratio is the effective efficiency of absorbing the inner bremsstrahlung photons. Multiplying that ratio by equation 3.13 gives the effective radiative correction. Comparing all three radiative corrections can be seen in figure 3.3

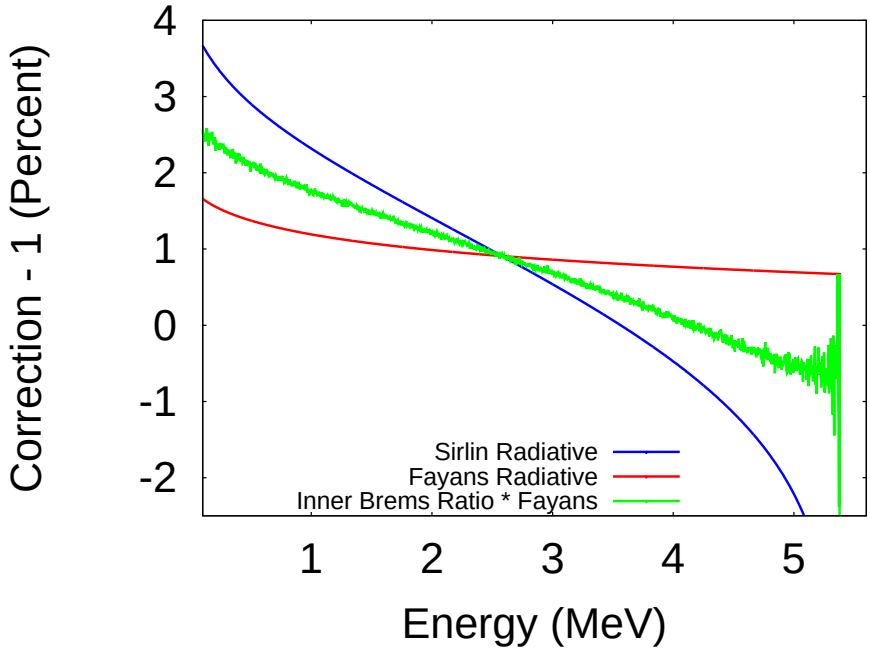

Figure 3.3: Comparing three different radiative corrections. The green line depends strongly on the detector geometry.

In order to see the effect of each correction on the slope, all three corrections offset in order to start from the same starting point. This is seen in figure 3.4. The effect of the inner

bremsstrahlung is to put the radiative correction halfway between the Sirlin and the Fayans formulas.

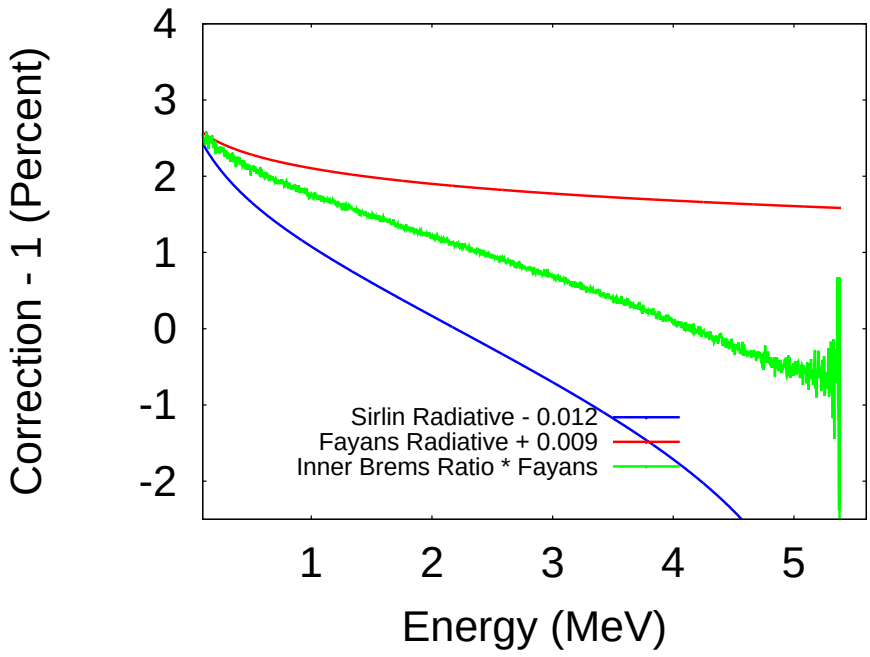

Figure 3.4: Starting all three radiative corrections from the same place. The green line is about halfway between the two others.

3.4.3 Screening

The screening correction is the next largest electromagnetic correction. It corresponds to the screening of the nuclear charge due to the electron cloud of the atom. The strongest effect of the screening correction is at low electron energies. This is a correction to the Fermi function.

3.4.3.1 Potentials Used in Screening Derivation

To calculate this correction, the Coulomb potential used to calculate the Fermi function is replaced with a Hulthén potential. This is shown in equation 3.15

$$V(r) = -\frac{\alpha Z \beta}{e^{\beta r} - 1} \tag{3.15}$$

Where r is the distance away from the center and β is a parameter characterizing the diffuseness of the electron cloud. The ratio of this new Fermi function to the old Fermi function is the screening correction. It multiplies the phase space.

The screening correction is negligible expect for near the origin. Near the origin, equation 3.15 behaves as equation 3.16

$$V(r) = -\frac{\alpha Z}{r} + \frac{1}{2}\alpha Z \beta \tag{3.16}$$

and β is given by equation 3.17 [4].

$$\beta = 2C(Z)\alpha Z^{\frac{1}{3}} m_e \tag{3.17}$$

In the case of beta decay, the Z is number electrons of the mother atom. The assumption is that beta decay is occurring from neutral mother atoms. The only unknown is $C(Z)$.

To find the value of $C(Z)$, a comparison to another method of treating screening is needed. In another method of describing screening, the potential is described as a series of exponentials. This is shown in 3.18 [5].

$$V(r) = -\frac{\alpha Z}{r} \sum_n c_n e^{-b_n x} \tag{3.18}$$

where b_n and c_n are constants. The sum of all the c_n adds up to one. The value of x is shown in equation 3.19 [5]

$$x = 1.13\alpha Z^{\frac{1}{3}} r m_e \tag{3.19}$$

When equation 3.18 is expanded near the origin, the result is equation 3.20

$$V(r) = -\frac{\alpha Z}{r} + \alpha Z 1.13 \alpha Z^{\frac{1}{3}} m_e \sum_n b_n c_n \tag{3.20}$$

By comparing equation 3.16, equation 3.17 and equation 3.20, the results in equation 3.21 are obtained.

$$C(Z) = 1.13 \sum_n c_n b_n \tag{3.21}$$

For fluorine, $n = 1$, $c = 1$, and $b = 0.907$ [5].

3.4.3.2 Screening Correction Formula

With all these factors out of the way, the screening correction can be written. $C(Z)$ in equation 3.17 is $0.907 * 1.13 = 1.02491$. The result is shown in equation 3.22 [4].

$$Q(Z,W) = X(\frac{W'}{W})|\frac{\Gamma(\gamma + iy')}{\Gamma(\gamma + iy)}|^2 |\frac{\Gamma(\gamma + 2i\frac{p'}{\beta})}{\Gamma(\gamma + 2i\frac{p}{\beta})}|^2 e^{-\pi y} (\frac{2p}{\beta})^{2(1-\gamma)} \tag{3.22}$$

with $y = \frac{\alpha Z W}{p}$, $y' = \frac{\alpha Z W'}{p'}$,$\gamma$ is in table 3.1, $W' = W - \frac{1}{2}\alpha Z \beta$, and $p' = \frac{1}{2}p + \frac{1}{2}\sqrt{p^2 - 2\alpha Z W' \beta}$.

$X(\frac{W'}{W})$ is in equation 3.23

$$X = \frac{1 + \frac{W'+\gamma m}{W'}\frac{\beta}{p}^2 + \frac{1}{2}\gamma^2[1 + (1 - \frac{\alpha Z}{\beta(W+m)})^{\frac{1}{2}}]^{-2}\frac{W-m}{W'}\frac{\beta}{p}^2[1 - \frac{1-\gamma}{8\gamma}\frac{\beta}{p}^2]}{(1 + \frac{\beta}{4p}^2)} \tag{3.23}$$

The factor X in equation 3.23 is very close to 1. This correction matters most at low energy, and is very flat above 100 keV.

3.4.4 Finite Mass Correction

The finite mass correction corrects for the recoil movement of the ^{20}F nucleus. The form of finite mass corrections is given in equation 3.24 [27]

$$R(W, W_0, M) = 1 + r_0 + \frac{r_1}{W} + r_2 W + r_3 W^2 \tag{3.24}$$

With W being the total electron energy, W_0 the maximum electron energy, and M the nuclear bass of ^{20}Ne. The form of the r_i depends on if the decay is a vector decay or an axial decay. This is due to angular momentum conservation. Since ^{20}F is an axial decay, the form of the finite mass correction is shown in equations 3.25

$$\begin{aligned} r_0 &= -\frac{2W_0}{M} - \frac{W_0^2}{6M^2} - \frac{77}{18M^2} \\ r_1 &= -\frac{2}{3M} + \frac{7W_0}{9M^2} \\ r_2 &= \frac{10}{3M} - \frac{28W_0}{9M^2} \\ r_3 &= \frac{88}{9M} \end{aligned} \tag{3.25}$$

This effect is different that the hadronic shape factor.

3.4.5 Finite Size Correction

The finite size correction originates from treating the nucleus as a sphere uniformly charged sphere instead of a point particle. This sphere has a radius of R, as shown in equation 3.4. The form of the finite size correction is shown in equation 3.26 [27]

$$L_0(Z,W) = 1+\frac{13(\alpha Z)^2}{60}-\alpha ZWR\frac{41-26\gamma}{15(2\gamma-1)}-\alpha ZR\gamma\frac{17-2\gamma}{30W(2\gamma-1)}+a_{-1}\frac{R}{W}+\sum_{n=0}^{5}a_n(WR)^n+0.41(R-0.016 \tag{3.26}$$

Where the a_i coefficients are parameterized by equation 3.27

$$a = \sum_{x=1}^{6} b_x(\alpha Z)^x \tag{3.27}$$

The b_x coefficients are numbers shown in table 3.2

Table 3.2: Coefficients for finite mass correction

	b_1	b_2	b_3	b_4	b_5	b_6
a_{-1}	0.115	-1.8123	8.2498	-11.223	-14.854	32.086
a_0	-0.00062	0.007165	0.01841	-0.053736	1.12691	-1.5467
a_1	0.02482	-0.05975	4.84199	-15.3374	23.9774	-12.6534
a_2	-0.14038	3.64953	-38.8143	172.1368	-346.708	288.7873
a_3	0.008152	-1.15664	49.9663	-273.711	657.6292	-603.7033
a_4	1.2145	-23.9931	149.9718	-471.2985	662.1909	-305.6804
a_5	-1.5632	33.4192	-255.1333	938.5297	-1641.2845	1095.358

3.4.6 Convolution of Lepton and Nucleon Wavefunction

This is the last of the relevant electromagnetic corrections. In figure 3.2, the name given is, "convolution PS." This correction $C(Z,W)$ accounts for the interaction of the lepton

and nucleon wavefunctions. The radial part of the nucleon wavefunctions are modelled as a rectangle with width R. This is adequate for a shape measurement. Much like the finite size and mass corrections, this correction depends on the type of β decay. Since the decay of interest is an axial vector decay, the form of this correction is shown in equation 3.28

$$C(Z,W) = 1 + C_0 + C_1 W + C_2 W^2 \tag{3.28}$$

where the C coefficients are defined in equation 3.29 [27]

$$\begin{aligned} C_0 &= -\frac{-233(\alpha Z)^2}{630} - \frac{(W_0 R)^2}{5} + \frac{2\alpha Z R W_0}{35} \\ C_1 &= -\frac{21\alpha Z R}{35} + \frac{4W_0 R^2}{9} \\ C_2 &= -\frac{4R^2}{9} \end{aligned} \tag{3.29}$$

This correction depends on both the maximum energy of the outgoing electron and the charge radius. The shape contribution from this correction is minimal.

3.4.7 Hadronic Corrections

Nuclear form factors are one of the largest corrections to the beta spectrum. There are four relevant form factors that come together into a correction called here the nuclear shape factor The form factors are described in table 3.3 [17] [6]

$$S(E) = 1 + C_0 + C_1 + \frac{C_{-1}}{E} + C_2 E^2 \tag{3.30}$$

where the C terms depend on the form factors and nuclear decay variables. How the

Table 3.3: Nuclear Form Factors

Form Factor	Name	Value
c_{1nuc}	Fermi matrix element	0.253
c_{2nuc}	Matrix element momentum transfer factor	0.755 fm^2
b_{wm}	Weak magnetism	43.4
d	Induced tensor term	40.5

shape factor depends on the form factors is shown in equation 3.31 [6]

$$\begin{aligned} c_0 &= -\frac{2E_0}{M_{ave}}(1+\frac{d}{c_{1nuc}}+\frac{b_{wm}}{c_{1nuc}})+\frac{2c_{2nuc}}{9c_{2nuc}}11m_e^2 \\ c_{-1} &= -\frac{m_e^2}{3M_{ave}}(2+\frac{2b_{wm}}{c_{1nuc}}+\frac{d}{c_{1nuc}})-\frac{2c_{2nuc}}{9c_{1nuc}}2m_e^2E_0 \\ c_1 &= \frac{2}{3M_{ave}}(5+\frac{b_{wm}}{c_{1nuc}})+\frac{2c_{2nuc}}{9c_{1nuc}}20E_0 \\ c_2 &= -\frac{40c_{2nuc}}{9c_{1nuc}} \end{aligned} \tag{3.31}$$

Two of the form factors, b_{wm} and c_{1nuc} are calculated from experimental data. d and c_{2nuc} are calculated from nuclear theory. The calculation of c_{1nuc} depends on the ft value. The calculation is shown in equation 3.32 [17]

$$c_{1nuc}^2 = \frac{2ft_0}{ft_{20}} \tag{3.32}$$

Where ft_0 is the ft value of the Fermi superallowed β decays, and ft_{20} the average of the ft values of the decays of ^{20}F and ^{20}Ne. This gives a value of 0.254 ± 0.004 [17]. The weak magnetism ,b_{wm}, is of special theoretical interest.

3.4.7.1 The Weak Magnetism

The other form factor from the data is the weak magnetism form factor. It can be calculated from a $M1$ analog gamma-ray decay strength. This decay strength is from the 10.275 MeV analog state to the 1.634 MeV first excited state in ^{20}Ne. This is a 2^+ to 2^+ angular momentum transition, and a 1 to 0 isospin transition. The decay strength, Γ_{M1}, can be used to calculate b_{wm} as shown in equation 3.33

$$b_{wm} = \sqrt{\frac{6\Gamma_{M1}M^2}{\alpha E_\gamma^3}} \tag{3.33}$$

where M is the nuclear mass and E_γ the energy of that gamma ray. This gives a value of 43.4± 1.2 [17].

Getting a measurement of this value is of interest for two reasons. One, it tests the Conserved Vector Current (CVC) hypothesis. This hypotheis states that the weak interaction possesses a universal strength and a universal $V - A$ form [9]. This means that the quantity b_{wm} relates to difference of the magnetic moments of the neutron and the proton. In decays involving a $T = 1$ multiplet, the equation refeq:bwmcal is valid. This means the largest of the nuclear corrections can be determined from experimental data, which has a much smaller uncertainty than any theory calculations. The second reason is more experimental. It gives a parameter with which to benchmark analysis techniques. If the analysis produces a reasonable value of b_{wm}, the same procedure should give a good value for b_{gt}.

3.4.7.2 The Induced Tensor Form Factor

From equation 3.31, the induced tensor form factor d contributes to the corrections much in the same way as the Fierz term. The induced tensor form factor is calculated with theory.

Equation 3.34 gives the the tensor form factor [6]

$$d = Ag_A M_{\sigma L} \tag{3.34}$$

where A is the mass number (20 in this case), g_A the axial vector coupling constant, and $M_{\sigma L}$ a matrix element of the decay. This matrix element is shown in equation 3.35

$$M_{\sigma L} =< \beta||\tau^+ i\vec{\sigma} \times \vec{l}||\alpha > \tag{3.35}$$

where β is the final state, τ^+ the isospin raising operator, $\vec{\sigma}$ the spin operator, $\vec{l}$ the angular momentum operator, and α the initial state. [6] In order to get the initial and final states α and β, shell model calculations have to be used. Different calculations have found d to equale 40.5 [6] and 20.5 [17]. Since d is divided by the aveage nuclear mass, this uncertainty in the form factor will not cause a large systematic effect.

3.5 Summary

With all these corrections, the experiment can be described to the required percision. The next chapter will describe details of the experimental set up and the detector configuration.